IET Radar, Sonar & Navigation

Research Article

IET Journals
The Institution of Engineering and Technology

Communication-embedded OFDM chirp waveform for delay-Doppler radar

ISSN 1751-8784
Received on 15th August 2017
Revised 6th November 2017
Accepted on 25th November 2017
E-First on 3rd January 2018
doi: 10.1049/iet-rsn.2017.0369
www.ietdl.org

MengJiao Li[1], Wen-Qin Wang[1] ✉, Zhi Zheng[1]

[1]Department of Communication and Information Engineering, University of Electronic Science and Technology of China, No. 2006 XiYuan Ave, West Hi-Tech Zone, Chengdu, People's Republic of China

✉ *E-mail: wqwang@uestc.edu.cn*

Abstract: A fundamental problem in the fusion of wireless communications and radar is to design suitable waveforms that can be simultaneously used for information transmission and radar sensing. In this study, the authors extend the orthogonal frequency division multiplexing (OFDM) waveform by embedding communication codes to communication-embedded OFDM chirp waveforms for delay-Doppler radar applications. The waveforms are characterised by jointly utilising the advantages of classic phase modulation in communications and chirp frequency modulation in high-resolution radar. The integrated radar-communication system scheme is formulated, which can operate as wireless communications and delay-Doppler radar simultaneously. In a generic monostatic radar setting, a closed-form expression is derived to evaluate the ambiguity function of the designed waveforms, along with the average and variance analysis of the ambiguity function.

1 Introduction

Along with technological development, integrating radar and communication is becoming increasingly necessary owing to that radar and wireless communications have more and more similar radio frequency (RF) front-end architectures [1, 2] and greater demand on bandwidth against strictly finite RF electromagnetic spectrum resource [3–5]. By using a joint waveform for both applications, the occupied spectrum would be used very efficiently and both applications could operate simultaneously. There is thus a large area of applications which would possibly benefit from the availability of integrated radar-communication systems [6–10]. Embedding communication information into radar emission was investigated in [1] by radiating one waveform during each radar pulse from a set of pre-designed waveforms. However, changing the waveform from pulse to pulse may degrade the radar performance. We can see that the main challenge in integrated radar-communication implementation lies in finding suitable waveforms that can be simultaneously used for information transmission and radar sensing. Although waveform design has received much recognition, especially in multiple-input multiple-output (MIMO) radar area [11], communication-embedded radar waveform design received relative few attentions. A null space projection method was proposed in [12] to exploit the spatial diversity provided by MIMO radars to direct the main beam into the null subspace of the communication channel matrix. A dynamic spectrum allocation approach was proposed in [13] for the coexistence of a radar system with a communication system. The authors developed a combined mutual information criterion for the joint waveform and power spectrum design to optimise the radar-communication performance.

Classical radar waveform design aims at creating the waveforms with optimum autocorrelation properties. The most popular example fulfilling this requirement is the chirp waveform. An intuitive approach for designing an integrated radar-communication waveform is to use chirp modulation for encoding the data. Up-chirp linearly frequency modulation (LFM) and down-chirp LFM were used in [14] for communication and radar functions, respectively, but it achieves low communication symbol rate corresponding to the chirp rate only [1]. In [15], different Oppermann sequences were employed for integrated radar-communication systems. These two waveforms have to be separated first from the receiver before executing further signal processing. In [16], another radar-communication waveform by modulating frequency modulated continuous-wave waveform with amplitude shift keying (ASK) was adopted, but it has poor peak-to-average power ratio (PAPR) performance due to the amplitude modulation. In order to achieve better communication performance in term of the symbol rate, continuous transmit signals should be employed [2]. A typical communication waveform with good autocorrelation properties is the spread spectrum signal [17, 18], but it is not suitable for radar applications due to its limited time-bandwidth product and low frequency efficiency [19].

Orthogonal frequency division multiplexing (OFDM) is a popular choice for integrated radar-communication waveform because it offers advantages such as robustness against multipath fading and relative simple synchronisation [20–25]. Time and frequency synchronisation is crucial in OFDM communications to preserve the orthogonality of the subcarriers. For radar, however, sensitivity to synchronisation is beneficial since radar uses a stored version of the transmitted signal and measures the time-delay and frequency offsets between the transmitted signal and received returns to estimate the range and closing velocity of a target [26]. It was pointed out in [27] that OFDM-coded radar signals are comparable with LFM waveforms without range-Doppler coupling. However, traditional OFDM communication signals usually have high PAPR [28]. Variations on the waveform envelope require using linear amplifiers on the transmit side. Moreover, to prevent the waveform from getting clipped by the amplifier, the waveform's peak power must be lower than the amplifier's 1 dB compression point. Such an arrangement leads to the inefficient transmitter. As chirp waveform has been widely used in practical radar systems due to its attractive properties [29], a novel OFDM chirp waveform design scheme was proposed in [30]. Although it can be easily extended to generate more than two waveforms, the waveforms will generate large grating lobes. We proposed OFDM chirp waveforms [11, 31], in which only radar applications are considered. It is shown that the OFDM chirp waveform has comparable performance with classic chirp signals and furthermore experiences no range-Doppler coupling problem.

In this paper, we extend the OFDM chirp waveform by embedding phase modulated communication information for delay-Doppler radar. The waveform is characterised by jointly utilising the advantages of classic phase modulation in communications and large time-bandwidth product chirp frequency modulation in high-resolution radar. In doing so, the communication-embedded OFDM

chirp waveform could have good PAPR and large time–bandwidth product. Relative to our previous publications [11, 18, 32, 33], the contributions of this work can be summarised as follows:

(i) Communication information via phase modulation is embedded into the OFDM chirp waveform without degrading the waveform ambiguity function characteristics for delay-Doppler radar applications. Based on this waveform, an integrated radar-communication system scheme is formulated.
(ii) Different from the OFDM chirp radar using the same waveform for all pulse durations, in the communication-embedded OFDM chirp radar, distinct waveforms should be transmitted in different pulse duration to embed communication information. Furthermore, a closed-form expression is derived to evaluate the radar ambiguity function of the waveforms. The waveform performances are comparatively evaluated with conventional OFDM waveform by examining the radar ambiguity function for radar applications and bit error rate (BER) for communications.

The remaining of this paper is organised as follows. Section 2 proposes the communication-embedded OFDM chirp waveform and presents the integrated radar-communication system scheme. Section 3 derives the closed-form expression of the ambiguity function, along with the average and variance analysis. Next, numerical results are provided in Section 4. Finally, concluding summaries are drawn in Section 5.

2 Communication-embedded OFDM chirp system design

To illustrate the proposed communication-embedded OFDM chirp waveform is suitable for implementation of integrated radar and communication system, in this section we first introduce the newly designed waveform and then present the system scheme.

2.1 Communication-embedded OFDM chirp waveform

The communication-embedded OFDM chirp waveform is proposed based on the existing OFDM chirp radar waveform. Suppose each waveform consists of Q subchirp signals, the ith existing OFDM chirp radar waveform can be represented by

$$u_i(t) = \sum_{q=0}^{Q-1} b_{i,q} \mathrm{e}^{\mathrm{j}2\pi c_{i,q}\Delta f t + \mathrm{j}\pi k_r t^2} s(t - q\Delta t), \tag{1}$$

where $b_{i,q}$ is the subchirp amplitude, $c_{i,q}$ is the subcarrier frequency index, Δf is the subchirp bandwidth as well as the frequency hopping interval, k_r is the subchirp rate, and $s(t) = 1, 0 < t < \Delta t$ with Δt being the hopping interval. Accordingly, the subchirp starting frequency is determined by $c_{i,q}\Delta f$.

The waveform design amounts to optimally choosing $b_{i,q}$ and $c_{i,q}$. Assuming M waveforms should be designed, we can then arrange $b_{i,q}$ and $c_{i,q}$ into $M \times N_s$ (N_s denotes the number of symbols) dimensional amplitude matrix $\boldsymbol{B}$ and code matrix $\boldsymbol{C}$, respectively. Optimisation techniques can be adopted to further improve the waveform orthogonality. An efficient approach is to optimise the amplitude matrix $\boldsymbol{B}$ and code matrix $\boldsymbol{C}$ through sparse modelling and subsequent correlation optimisation with simulated annealing algorithm [32].

In radar application, both the amplitude matrix $\boldsymbol{B}$ and code matrix $\boldsymbol{C}$ can be optimised to achieve improved system performance. However, if integrated radar-communication applications are expected, similar optimisation techniques cannot be employed for the waveform design, because the waveform amplitude and phase should have a direct relation with the transmitted communication information and should be used for information transmission. Otherwise, the communication information cannot be efficiently embedded in the radar waveform.

When communication information is embedded, the OFDM chirp waveform can be regarded as a parallel stream of multiple chirp signals with orthogonal subcarriers, each modulated with different transmit data. Consider a communication-embedded OFDM chirp waveform with N_c subcarriers and let $a(n)$ denote the discrete amplitude and phase states obtained through any communication modulation scheme. Then, a communication-embedded OFDM chirp pulse is

$$u(t) = \sum_{n=0}^{N_c-1} a(n)\exp\left(\mathrm{j}2\pi f_n t + \mathrm{j}\pi k_r t^2\right)\mathrm{rect}\left(\frac{t - T_\mathrm{w}}{T_\mathrm{w}}\right), \tag{2}$$

where f_n is the individual subcarrier starting frequency, $T_\mathrm{w} = T + T_\mathrm{g}$ denotes the whole OFDM symbol duration including an elementary symbol duration T and a guard interval cyclic prefix duration T_g corresponding to the maximum expected time delay and $\mathrm{rect}(t/T_\mathrm{w})$ describes a rectangular window with duration T_w. Suppose each signal frame is composed of N_s OFDM chirp modulation symbols, the transmitted signal can then be expressed as

$$x(t) = \sum_{m=0}^{N_s-1}\sum_{n=0}^{N_c-1} a(mN_c + n)\exp\left(\mathrm{j}2\pi f_n t + \mathrm{j}\pi k_r t^2\right) \cdot \mathrm{rect}\left(\frac{t - mT_\mathrm{w}}{T_\mathrm{w}}\right), \tag{3}$$

where m denotes the individual OFDM chirp symbol index within the N_s symbols.

Similarly, in order to ensure the subcarrier orthogonality, f_n should hold as

$$f_n = n\Delta f = \frac{n}{T}, \quad n = 0, 1, \ldots, N_c - 1. \tag{4}$$

The cyclic prefix is widely employed in an OFDM communication to deal with inter-symbol interferences due to multipath propagation [34]. In radar applications, the response of each range cell will be a summation of the responses of all scatterers within this range cell. Thus, in order to convert these interfered range cells to individual range cells without inter-range-cell interferences [35], similar to OFDM communication systems, the cyclic prefix length also should be longer than the desired maximum time-delay.

For instance, if D range cell paths are superposed together in the radar returned signal, the guard interval length T_g in the analogue transmission signal should be $T_\mathrm{g} = (D-1)T_\mathrm{s}$ with T_s being the sampling interval at the receiver. Since $T = N_c T_\mathrm{s}$, the total OFDM chirp symbol duration T_w should be $T_\mathrm{w} = T + T_\mathrm{g} = (D + N_c - 1)T_\mathrm{s}$. A partial cyclic repetition of the time-domain signal of the duration T_g can be used for the cyclic prefix, which is typically prepended at the beginning of the symbol, occupying the interval $[0, T_\mathrm{g})$ within the total symbol duration T_w. In doing so, the receiver only evaluates the interval $[T_\mathrm{g}, T_\mathrm{w})$ to avoid the inter-range-cell interference.

In order to not destroy the orthogonality of the subcarriers, the subcarrier spacing Δf should be much larger than the maximum Doppler shift f_{D_max}. On the other hand, Δf has an influence on the achievable range resolution, which is an important radar performance parameter. The range resolution depends neither on the employed waveform nor on the particular system parameters but only on the total bandwidth occupied by the transmitted signal. Here, the range resolution is

$$\rho_r = \frac{c_0}{2N_c\Delta f}, \tag{5}$$

where c_0 is the speed of light. In typical radar applications, the range resolution should be in the order of 1–2 m and the required total bandwidth is over 100 MHz. This is compliant with the regulations for 24 GHz industrial, scientific and medical band. Furthermore, the OFDM symbol duration T should be chosen as long as possible to obtain a sufficient high signal-to-noise ratio (SNR) for the received signals. However, the guard interval

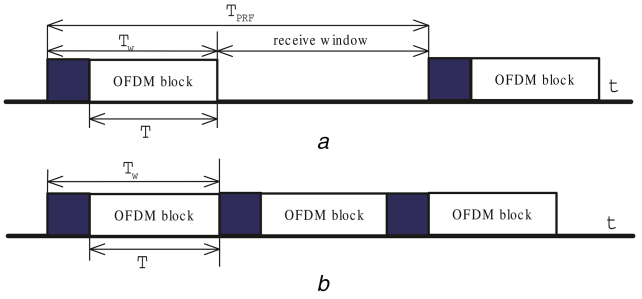

Fig. 1 *Comparisons between traditional OFDM radar and communication-embedded radar*

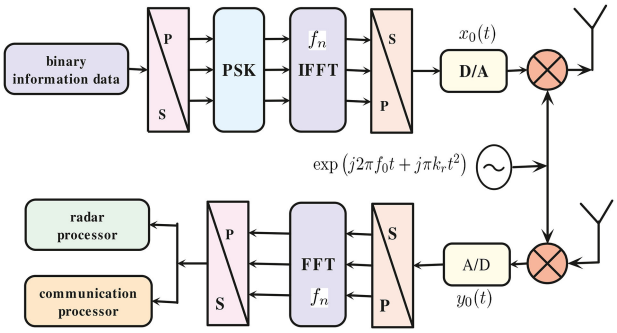

Fig. 2 *Block scheme of integrated radar-communication system*

duration T_g and symbol duration T are limited by the maximum unambiguous velocity measurement

$$v_{\max} = \frac{c_0}{(T + T_g) f_0}. \tag{6}$$

Hence, a trade-off should be made in the system design.

2.2 Integrated radar-communication system scheme

In standard OFDM radar applications, the transmitted signals and returned signals are usually separated in time due to the fact that in a monostatic case the transmitter and receiver share the same antenna and cannot transmit and receive signals simultaneously. This implies that a reasonable receiving window is needed between two consecutive pulses, as shown in Fig. 1*a*. In order to achieve high transmission throughput for the communications, here, the communication-embedded OFDM chirp pulses are transmitted consecutively, as shown in Fig. 1*b*. Accordingly, separated transmit and receive antennas are assumed, so that the system can transmit and receive signals simultaneously. Considering that the location of transmit and receive antennas is often furnished closely, the transmitted signal will produce strong self-interference to the receiving end, making the receiver unable to extract the useful signal. Since the key technology of full-duplex communication is self-interference suppression and cancellation, there exists a lot of solutions for this issue. Specially, we recommend the interference cancellation method for OFDM system that was proposed in [36]. It is reported that 80 dB transmitter–receiver isolation has been achieved.

The communication-embedded OFDM chirp modulation and demodulation can be similarly implemented as conventional OFDM communications. Fig. 2 illustrates the block scheme of the integrated radar-communication system. First, the binary communication data are divided into parallel streams via serial-to-parallel (S/P) conversion, and mapped into complex-valued modulation symbol sequences $d_T(m, n)$. Phase-shift keying (PSK) and quadrature amplitude modulation (QAM) are two popular modulation techniques widely employed in OFDM communication systems. However, since amplitude modulation is employed in QAM but only phase modulation is applied in PSK, we recommend PSK for this radar-communication system, so that lower PAPR level can be achieved for the system. During the modulation, OFDM symbols are typically divided into frames, so that the data will be modulated frame by frame to make the received signal synchronisation with the receiver. The standard OFDM time-domain waveform $x_0(t)$ can be obtained by a block-wise inverse discrete Fourier transform and subsequent parallel-to-serial (P/S) and digital-to-analogue (D/A) conversions

$$x_0(t) = \sum_{m=0}^{N_s-1} \sum_{n=0}^{N_c-1} a(mN_c + n) \exp(\mathrm{j}2\pi f_n t) \mathrm{rect}\left(\frac{t - mT_w}{T_w}\right). \tag{7}$$

Since the inverse fast Fourier transform can be effectively implemented, it is usually used instead. Once the OFDM data are modulated to time-Doppler signal, all carriers fully occupy the available frequency bandwidth. Finally, after being mixed with a local oscillator (LO) signal

$$x_{\mathrm{LO}}(t) = \exp\left(\mathrm{j}2\pi f_0 t + \mathrm{j}\pi k_r t^2\right) \mathrm{rect}\left(\frac{t - mT_w}{T_w}\right), \tag{8}$$

with a carrier frequency f_0, the generated OFDM chirp signal is radiated towards the desired region. Note that the main implementation difference between our OFDM chirp and standard OFDM methods in this system scheme lies in that the former uses $\exp\left(\mathrm{j}2\pi f_0 t + \mathrm{j}\pi k_r t^2\right)\mathrm{rect}((t - mT_w)/T_w)$ as the LO signal to achieve lower PAPR to facilitate the subsequent RF amplifier design, while the latter uses $\exp(\mathrm{j}2\pi f_0 t)\mathrm{rect}((t - mT_w)/T_w)$ as the LO signal.

In the receiver, the same steps are carried out in an inverse order. The cyclic prefix allows the demodulator to capture the symbol period with an uncertainty up to the cyclic prefix length and still obtain the correct information for the entire period. The cyclic prefix allows the receiver to capture the starting point of a symbol period, such that the result of fast Fourier transform (FFT) has the correct information. After de-chirped by the LO signal $x_0(t) = \exp\left(\mathrm{j}2\pi f_0 t + \mathrm{j}\pi k_r t^2\right)\mathrm{rect}((t - mT_w)/T_w)$, the received modulation symbols $d_R(m, n)$ can be recovered from the received baseband signal by an FFT operation.

The returned signal from a reflecting object at the distance R can be expressed as

$$\begin{aligned} y(t) = \sum_{m=0}^{N_s-1} \sum_{n=0}^{N_c-1} & \exp\left(\mathrm{j}2\pi f_n\left(t - \frac{2R}{c_0}\right) + \mathrm{j}\pi k_r\left(t - \frac{2R}{c_0}\right)^2\right) \\ & \times A(m, n) d_T(m, n) \exp(\mathrm{j}2\pi f_{\mathrm{d}} t) \mathrm{rect}\left(\frac{t - kT_w - (2R/c_0)}{T_w}\right), \end{aligned} \tag{9}$$

where $A(m, n)$ is the complex amplitude describing the attenuation and phase shift due to the propagation and scattering process and f_{d} is the Doppler shift. Note that, here, we consider only the baseband signal and ignore the carrier frequency associated terms, which will be cancelled out by the RF mixer and corresponding phase compensating algorithm. At the same time, the receiver recovers the individual modulation symbols for the communication functionality by observing the received signal for only the elementary OFDM chirp symbol duration T. This implies that, when the guard interval duration T_g is properly designed, we can cut the observed samples and accordingly the time shift of rect(·) in (13) can be neglected. In this case, (13) can be represented by

$$\begin{aligned} y_0(t) = \sum_{m=0}^{N_s-1} \sum_{n=0}^{N_c-1} & A(m, n) d_T(m, n) \exp\left(\mathrm{j}2\pi f_n\left(t - \frac{2R}{c_0}\right)\right) \\ & \times \exp(\mathrm{j}2\pi f_{\mathrm{d}} t) \mathrm{rect}\left(\frac{t - kT_w}{T_w}\right), \end{aligned} \tag{10}$$

where we assume the chirp rate k_r associated terms have been cancelled or compensated in the dechirp-on-receive operation [37]. At this step, $y_0(t)$ is equal to the received signal in the standard OFDM communication system and thus, the transmitted information can be simply recovered by classic OFDM communication algorithms.

3 Averaged ambiguity function analysis

When the OFDM signal bandwidth is much smaller than the carrier frequency, the Doppler frequency will result in an identical phase shift on each subcarrier. However, for a fixed subcarrier, it will cause a linear phase shift between consecutive modulation symbols on that subcarrier, corresponding to the phase change of the Doppler shift during the total transmitted OFDM symbol duration, namely, $2\pi f_{\mathrm{d}} T_{\mathrm{w}}$. More importantly, it has been pointed out in [2] that, the range and Doppler introduced by a reflecting object have a completely orthogonal influence on the modulation symbols. The range introduces a linear phase shift only along the frequency axis, whereas the Doppler introduces the phase shift along the time axis. Hence, it is possible to recover the range and Doppler independently with a suitable processing algorithm. We can adopt the range-Doppler estimation algorithm detailed in [22]. In this section, we derive the radar ambiguity function for the OFDM chirp waveform.

Radar ambiguity function fully characterises the radar discrimination capability in both range and velocity dimensions [38, 39]. The radar ambiguity function of a signal $x(t)$ is expressed as

$$\chi(\tau, f_{\mathrm{d}}) = \int_{-\infty}^{\infty} x(t) x^*(t-\tau) \mathrm{e}^{-\mathrm{j}2\pi f_{\mathrm{d}} t} \mathrm{d}t \,. \tag{11}$$

By substituting $x(t)$ with (3), we can get the ambiguity function of communication-embedded OFDM chirp waveform:

$$\begin{aligned}\chi(\tau, f_d) &= \int_{-\infty}^{\infty} x(t) x^*(t-\tau) \mathrm{e}^{-\mathrm{j}2\pi f_d t} \mathrm{d}t \\ &= \sum_m \sum_n \sum_{m'} \sum_{n'} a_{m,n} a^*_{m',n'} \int_{-\infty}^{\infty} \mathrm{e}^{\mathrm{j}2\pi n \Delta f t + \mathrm{j}\pi k_r t^2} \mathrm{rect}\left(\frac{t - mT_{\mathrm{w}}}{T_{\mathrm{w}}}\right) \\ &\quad \times \mathrm{e}^{-\mathrm{j}2\pi n' \Delta f (t-\tau) - \mathrm{j}\pi k_r (t-\tau)^2} \mathrm{rect}\left(\frac{t - \tau - m'T_{\mathrm{w}}}{T_{\mathrm{w}}}\right) \mathrm{e}^{-\mathrm{j}2\pi f_{\mathrm{d}} t} \mathrm{d}t,\end{aligned} \tag{12}$$

which ignores the propagation attenuation and target reflection coefficient that are ignorable to the ambiguity function analysis. Note that the summation limitations are omitted throughout the following derivations due to space constraints.

Different from conventional OFDM radar transmitting the same waveform in each pulse, in the communication-embedded OFDM radar distinct waveforms should be transmitted in different durations to embed the communication information. Analogous to [39–41], we use the averaged radar ambiguity function $\bar{\chi}(\tau, f_{\mathrm{d}})$ as a performance metric to evaluate the ambiguity function, due to also that it can generally evaluate the matched filter output for all waveforms with the same statistical properties. More importantly, a closed-form expression can be derived for the designed waveform, which is helpful for investigating the limitations of the designed waveforms and developing proper techniques to counteract their disadvantages. The average ambiguity function can be defined as [40, 42]

$$\bar{\chi}(\tau, f_{\mathrm{d}}) = \left| E\{\chi(\tau, f_{\mathrm{d}})\} \right|. \tag{13}$$

Assuming the symbols $a_{m,n}$ are statistically independent, we then have

$$E\{a_{m,n} a^*_{m',n'}\} = \begin{cases} \xi, & m = m', n = n' \\ 0, & \text{else} \end{cases} \tag{14}$$

where $\xi = 1/N_s N_c T_{\mathrm{w}}$ is a constant chosen so as to guarantee that $\int_{-\infty}^{\infty} |s(t)|^2 \mathrm{d}t = 1$. Substituting (14) into (13), we can get

$$\begin{aligned}\bar{\chi}(\tau, f_{\mathrm{d}}) &= \xi \left| \mathrm{e}^{-\mathrm{j}\pi k_r \tau^2} \sum_m \sum_n \mathrm{e}^{\mathrm{j}2\pi n \Delta f \tau} \int_{-\infty}^{\infty} \mathrm{rect}\left(\frac{t - mT_{\mathrm{w}}}{T_{\mathrm{w}}}\right) \right. \\ &\quad \left. \times \mathrm{rect}\left(\frac{t - \tau - mT_{\mathrm{w}}}{T_{\mathrm{w}}}\right) \mathrm{e}^{-\mathrm{j}2\pi (f_{\mathrm{d}} - k_r \tau) t} \mathrm{d}t \right| \\ &= \xi \left| \mathrm{e}^{-\mathrm{j}\pi k_r \tau^2} \cdot \int_{-\infty}^{\infty} \mathrm{rect}\left(\frac{t}{T_{\mathrm{w}}}\right) \mathrm{rect}\left(\frac{t - \tau}{T_{\mathrm{w}}}\right) \mathrm{e}^{-\mathrm{j}2\pi (f_{\mathrm{d}} - k_r \tau) t} \mathrm{d}t \right. \\ &\quad \left. \times \sum_m \mathrm{e}^{-\mathrm{j}2\pi (f_{\mathrm{d}} - k_r \tau) m T_{\mathrm{w}}} \sum_n \mathrm{e}^{-\mathrm{j}2\pi (f_{\mathrm{d}} - k_r \tau) m T_{\mathrm{w}}} \right|.\end{aligned} \tag{15}$$

According to the following relations:

$$\begin{aligned}\chi_{\mathrm{w}}(\tau, f_{\mathrm{d}}) &= \int_{-\infty}^{\infty} \mathrm{rect}\left(\frac{t}{T_{\mathrm{w}}}\right) \mathrm{rect}\left(\frac{t - \tau}{T_{\mathrm{w}}}\right) \mathrm{e}^{-\mathrm{j}2\pi f_d t} \mathrm{d}t \\ &= \frac{\sin \pi f_{\mathrm{d}} (T_{\mathrm{w}} - |\tau|)}{\pi f_{\mathrm{d}}}\end{aligned} \tag{16a}$$

$$\begin{aligned}\sum_{m=0}^{N_s - 1} \mathrm{e}^{-\mathrm{j}2\pi (f_{\mathrm{d}} - k_r \tau) m T_{\mathrm{w}}} &= \frac{1 - \mathrm{e}^{-\mathrm{j}2\pi (f_{\mathrm{d}} - k_r \tau) N_s T_{\mathrm{w}}}}{1 - \mathrm{e}^{-\mathrm{j}2\pi (f_{\mathrm{d}} - k_r \tau) T_{\mathrm{w}}}} \\ &= \mathrm{e}^{-\mathrm{j}\pi (N_s - 1) T_{\mathrm{w}}} \frac{\sin(\pi (f_{\mathrm{d}} - k_r \tau) N_s T_{\mathrm{w}})}{\sin(\pi (f_{\mathrm{d}} - k_r \tau) T_{\mathrm{w}})}\end{aligned} \tag{16b}$$

$$\sum_{n=0}^{N_c - 1} \mathrm{e}^{\mathrm{j}2\pi n \Delta f \tau} = \mathrm{e}^{\mathrm{j}\pi (N_c - 1) \Delta f \tau} \frac{\sin(\pi N_c \Delta f \tau)}{\sin(\pi \Delta f \tau)}, \tag{16c}$$

where $\chi_{\mathrm{w}}(\tau, f_{\mathrm{d}})$ is equal to the ambiguity function of a window function, the average of the ambiguity function can be finally derived as

$$\begin{aligned}E\{\chi(\tau, f_{\mathrm{d}})\} = \bar{\chi}(\tau, f_{\mathrm{d}}) &= \xi \left| \frac{\sin \pi (f_{\mathrm{d}} - k_r \tau)(T_{\mathrm{w}} - |\tau|)}{\pi (f_{\mathrm{d}} - k_r \tau)} \right| \\ &\quad \times \left| \frac{\sin(\pi (f_{\mathrm{d}} - k_r \tau) N_s T_{\mathrm{w}})}{\sin(f_{\mathrm{d}} - k_r \tau) T_{\mathrm{w}}} \right| \left| \frac{\sin(\pi N_c \Delta f \tau)}{\sin(\pi \Delta f \tau)} \right|\end{aligned} \tag{17}$$

Furthermore, the variance of the ambiguity function can be calculated by [42]

$$\sigma^2_{\chi}(\tau, f_{\mathrm{d}}) = E\left\{ |\chi(\tau, f_{\mathrm{d}})|^2 \right\} - |E\{\chi(\tau, f_{\mathrm{d}})\}|^2 . \tag{18}$$

After some lengthy but straightforward derivations (see Appendix), $E\left\{ |\chi(\tau, f_{\mathrm{d}})|^2 \right\}$ can be expressed as (19). Finally, by substituting $E\left\{ |\chi(\tau, f_{\mathrm{d}})|^2 \right\}$ and $E\{\chi(\tau, f_{\mathrm{d}})\}$ to (18), we get the variance of the ambiguity function (20) (see (19))

$$\begin{aligned}\sigma^2_{\chi}(\tau, f_{\mathrm{d}}) = &\sum_{m = -(N_s - 1)}^{N_s - 1} (N_s - m) \sum_{n = -(N_c - 1)}^{N_c - 1} (N_c - n \\ &) |\chi_{\mathrm{w}}(\tau - mT_{\mathrm{w}}, f_{\mathrm{d}} - n\Delta f + k_r \tau)|^2\end{aligned} \tag{20}$$

$$\begin{aligned}E\left\{ |\chi(\tau, f_{\mathrm{d}})|^2 \right\} = \xi^2 \left(\left| \frac{\sin \pi (f_{\mathrm{d}} - k_r \tau)(T_{\mathrm{w}} - |\tau|)}{\pi (f_{\mathrm{d}} - k_r \tau)} \right|^2 \left| \frac{\sin(\pi (f_{\mathrm{d}} - k_r \tau) N_s T_{\mathrm{w}})}{\sin(f_{\mathrm{d}} - k_r \tau) T_{\mathrm{w}}} \right|^2 \left| \frac{\sin(\pi N_c \Delta f \tau)}{\sin(\pi \Delta f \tau)} \right|^2 \right. \\ \left. + \sum_{m = -(N_s - 1)}^{N_s - 1} (N_s - m) \sum_{n = -(N_c - 1)}^{N_c - 1} (N_c - n) |\chi_{\mathrm{w}}(\tau - mT_{\mathrm{w}}, f_{\mathrm{d}} - n\Delta f + k_r \tau)|^2 \right).\end{aligned} \tag{19}$$

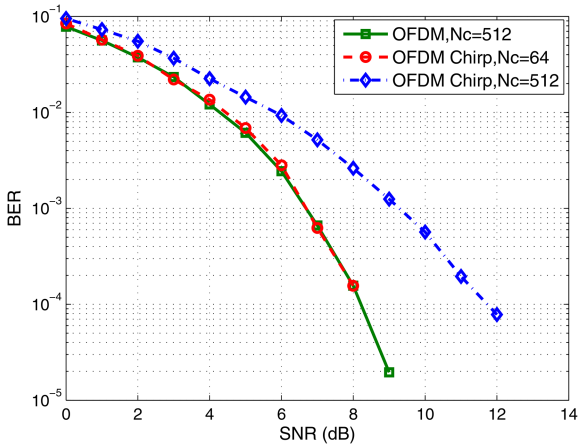

Fig. 3 *Comparisons of BER performance for OFDM and OFDM chirp*

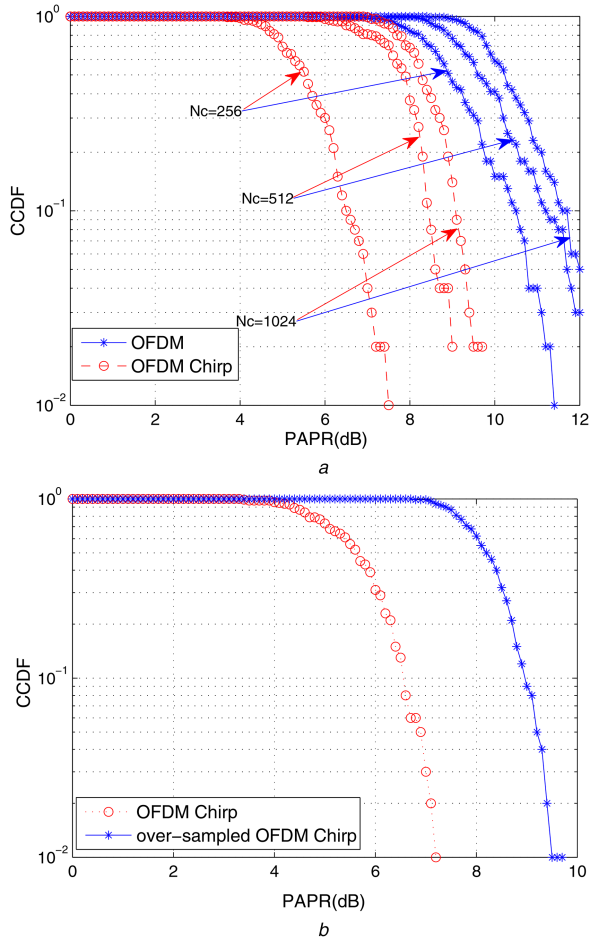

Fig. 4 *Comparisons of PAPR performance*
(a) Different subcarriers N_c, ***(b)*** Different oversampled rate

4 Simulation results and discussions

Radar performance emphasises detection, resolution and localisation capability, while communication performance focuses on data rate, error probability and coding efficiency. These performances have a direct relation with SNR. It is easily understood that the OFDM chirp waveform and standard OFDM waveform have an equal output SNR under the same condition. Furthermore, under the reasonable assumption that coding and modulation technology and channel bandwidth are the same, the two waveforms should have an approximately identical data rate. While in the receiver, BER performance varies because of different channel effect including noise and inter-carrier interference. The results of BER versus SNR are shown in Fig. 3, where 100 OFDM symbols have been calculated for the time averaging to count the bit error. The performance of OFDM waveform and the OFDM chirp waveform are compared in an AGWN channel condition. The bit data are generated randomly and modulated with BPSK. The guard interval is a quarter of the OFDM symbol length. The frequency modulation rate of the carrier of OFDM chirp waveform is 10 GHz/s. If only the guard interval length is large enough, the BER performance of traditional OFDM signal, the solid line marked with square in Fig. 3, will hold the line. The two BER curves of OFDM chirp waveform indicate that the performance will deteriorate with the increase of subcarrier number N_c. We also found that the BER curve will surge as the chirp rate increases. Obviously, the BER performance of an OFDM chirp waveform is inferior to that of the classic OFDM waveform.

PSK and QAM are two popular modulation techniques used in OFDM communication systems. QAM achieves higher spectra efficiency. However, since amplitude modulation is employed in QAM but only phase modulation is applied in PSK, we use PSK for the radar-communication system, so that lower PAPR level can be achieved for the system. The complementary cumulative density function (CCDF) is adopted here to assess the PAPR performance of the suggested waveform. The CCDF of PAPR denotes the probability that the PAPR of a data block exceeds a given PAPR threshold. Due to the fact that the real and imaginary parts of complex OFDM waveform obeys Gaussian distribution asymptotically, and thus, the amplitude of the signal obeys the Rayleigh distribution, we can get the theoretical distribution function of the CCDF of OFDM signal. For OFDM chirp signal, we cannot identify its amplitude distribution, so we do the Monte Carlo simulations by using 100 OFDM chirp blocks with random data to get the simulation result. The comparisons of PAPR curves are depicted in Fig. 4, which shows that the OFDM chirp waveform indeed achieves lower PAPR as OFDM waveform. Lower PAPR allows a more efficient transmitter. It is known that different subcarrier number and oversampled rate may lead to significant differences in the PAPR of OFDM waveform, so will they do to OFDM chirp waveform. As illustrated in Fig. 4*a*, the PAPR performance of both OFDM and OFDM chirp waveforms degrade along with the subcarrier number N_c increases, but OFDM chirp waveform achieves a lower PAPR level. To find the relationship between the PAPR of OFDM chirp waveform and its sampled sequence, we conducted eight times oversampling, which is much greater than the Nyquist-rate and the oversampling rates bound $\pi/\sqrt{2}$ introduced in [43]. The results shown in Fig. 4*b* indicate that PAPR will increase when the OFDM chirp signals are oversampled.

Next, we evaluate the use of the communication-embedded OFDM chirp waveform for radar delay and Doppler estimations. Suppose the following parameters: $N_c = 1024$, $\Delta f = 90.909\,\text{kHz}$, $k_r = 8.464 \cdot 10^{12}$, $R = 50\,\text{m}$, $T = 11\,\mu\text{s}$, $T_g = 1.375\,\mu\text{s}$, $A_{\text{OFDM}} = 100$. Fig. 5 compares the normalised range profiles for a point target between traditional correlation processing method and the modulation symbol-based processing method with the application of Hanning or Hamming window function. It is noticed that, undesired large sidelobes appear in the correlation processing method. This inherent property of OFDM signal is caused by the rectangular pulse shaping in OFDM transmitter. Besides, there are additional sidelobes at the range around 30 m, which is caused by internal correlations in the transmit data. Since the results are simulated with random data, it is expected that when transmitting real user data, the sidelobes may even increase. Furthermore, these sidelobes cannot be removed with a simple filter. In contrast, the modulation symbol-based processing method has no sidelobes resulting from rectangular pulse shaping and correlations within the user data, although the resolution width is widened due to the windowing effects.

Both communication and radar applications may be influenced by the waveform correlation characteristics. Fig. 6 compares the waveform auto-correlation characteristics. It is noticed that the OFDM chirp waveform produces better auto-correlation performance, which guarantees high dynamic measuring range for the matched filters in the receiver. In order to further evaluate the waveform characteristics, we analysed the ambiguity function performance. According to (13), the averaged ambiguity function

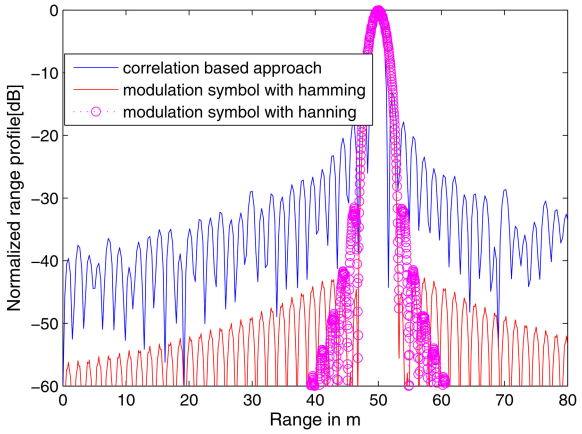

Fig. 5 *Comparisons of normalised range profiles*

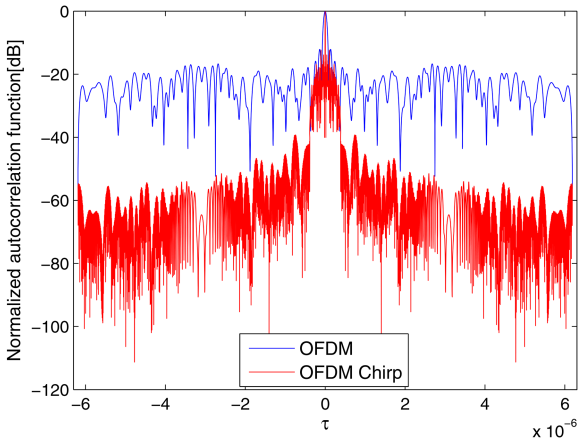

Fig. 6 *Comparisons of autocorrelation for OFDM and OFDM chirp*

of communication-embedded OFDM chirp waveform is shown in Fig. 7*a*, where the simulation parameters are as follows: $N_s = 8$, $N_c = 64$, $T = 20\,\mu$s, $T_g = 5\,\mu$s, $T_w = 25\,\mu$s, $B = 3.2$ MHz, $k_r = 1.25 \times 10^{11}$. The comparisons of their zero-Doppler cut profiles are provided in Fig. 7*b*. Note that, due to the employment of chirp signals in the waveform, the OFDM chirp waveform achieves a slightly better range resolution. It is apparent that OFDM chirp waveform achieves narrower mainlobe and lower sidelobe level than the standard OFDM waveform.

Suppose the OFDM chirp waveform has 10 symbols and 64 subcarriers. The variance of the corresponding ambiguity function is given in Fig. 7*c*, which shows zero variance in the centre and tiny amplitude fluctuations in other areas. The line ambiguity is the shift of the ambiguity function associated with the chirp waveform and determined by both the subcarrier index N_c and symbol index N_s.

Furthermore, Fig. 8 compares the ambiguity function with different N_s and/or N_c parameters. We can observe that the OFDM chirp ambiguity function resembles that of the classic LFM waveform because of the chirp signals adopted in its subcarriers. This means that the OFDM chirp waveform is non-sensitive to the Doppler shift. It is easily understood from Fig. 8 that the ambiguity area will reduce with the increase of N_s and N_c, which would also finally affect the range and velocity resolutions of the system. For instance, the zero-delay cut is dominated by $\sin(Nx)/\sin(x)$ [39], which yields a mainlobe width of $1/N_sT_w$ in the Doppler dimension. Apparently, a larger N_s implies a narrower mainlobe width. Therefore, we can conclude that the average ambiguity function of the OFDM chirp waveform does not depend on the particular baseband modulation, but is related to the OFDM signal modulation.

5 Conclusion

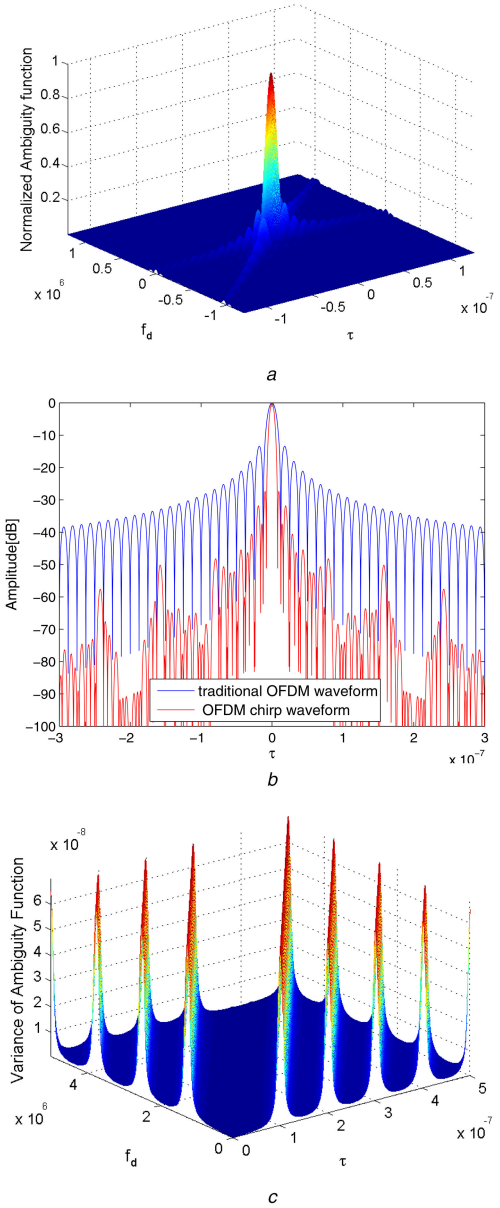

Fig. 7 *Numerical ambiguity function results*
(a) Ambiguity function of OFDM chirp waveform, ***(b)*** Comparisons of zero-Doppler cut, ***(c)*** Variance of ambiguity function of OFDM chirp waveform

This paper extended the OFDM chirp waveform by embedding communication codes for delay-Doppler radar. The waveform is characterised by jointly utilising the advantages of classic phase modulation in communications and chirp frequency modulation in high-resolution radar. The integrated radar-communication scheme is presented for simultaneous wireless communications and delay-Doppler radar applications. A closed-form expression for the averaged ambiguity function was derived, along with its average and variance analysis. Numerical results show that the OFDM chirp waveform can achieve higher radar resolution performance. Note that one antenna and one instantaneous communication-embedded OFDM chirp waveform are assumed in this paper. In future work, we plan to investigate the case with multiple antennas using instantaneous orthogonal communication-embedded OFDM chirp waveforms, where the challenge is to suppress the cross-correlation interferences between the waveforms.

6 Acknowledgments

This work was supported by the National Natural Science Foundation of China under grant no. 61571081, Young top-notch talent of the national Ten Thousand Talent Program, and Sichuan Technology Research and Development fund under grant no. 2015GZ0211.

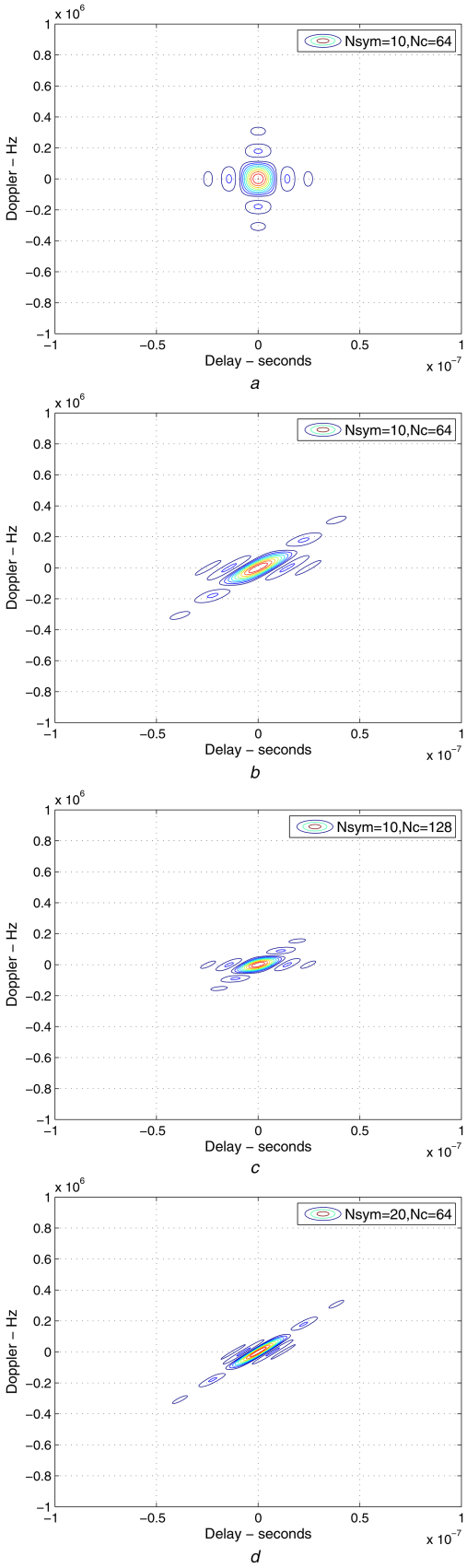

Fig. 8 *Contour plot of OFDM chirp waveform and traditional OFDM waveform*

(a) OFDM waveform with $N_{sym} = 10$, $N_c = 10$, ***(b)*** OFDM chirp waveform with $N_{sym} = 10$, $N_c = 64$, ***(c)*** OFDM chirp waveform with $N_{sym} = 10$, $N_c = 128$, ***(d)*** OFDM chirp waveform with $N_{sym} = 20$, $N_c = 64$

7 References

[1] Blunt, S.D., Yatham, P., Stiles, S.: 'Intra-pulse radar-embedded communications', *IEEE Trans. Aerosp. Electron. Syst.*, 2010, **46**, (3), pp. 1185–1200

[2] Sturm, C., Wiesbeck, W.: 'Waveform design and signal processing aspects for fusion of wireless communications and radar imaging', *Proc. IEEE*, 2011, **99**, (7), pp. 1236–1259

[3] Griffiths, H., Cohen, L., Watts, S., *et al.*: 'Radar spectrum engineering and management: technical and regulatory issues', *Proc. IEEE*, 2015, **103**, (1), pp. 85–102

[4] Bliss, D.W.: 'Cooperative radar and communications singaling: the estimation and information theory odd couple'. Proc. of IEEE Radar Conf., Cincinnati, OH, May 2014, pp. 50–55

[5] Hassanien, A., Amin, M.G., Zhang, Y.M., *et al.*: 'A dual function radar-communications system using sidelobe control and waveform diversity'. Proc. of IEEE Radar Conf., Arlington, VA, May 2015, pp. 1260–1263

[6] Chiriyath, A.R., Paul, B., Jacyna, G., *et al.*: 'Inner bounds on performance of radar and communications co-existence', *IEEE Trans. Signal Process.*, 2016, **64**, (2), pp. 464–474

[7] Hassanien, A., Amin, M.G., Zhang, Y.M., *et al.*: 'Dual-function radar-communications: information embedding using sidelobe control and waveform diversity', *IEEE Trans. Signal Process.*, 2016, **64**, (8), pp. 2168–2181

[8] Li, B., Petropulu, A.P., Trappe, W.: 'Optimum co-design for spectrum sharing between matrix completion based MIMO radars and a MIMO communication system', *IEEE Trans. Signal Process.*, 2016, **64**, (17), pp. 4562–4575

[9] Li, B., Petropulu, A.P., Trappe, W.: 'Analysis of symbol-design strategies for intrapulse radar-embedded communications', *IEEE Trans. Aerosp. Electron. Syst.*, 2015, **51**, (4), pp. 2914–2931

[10] Ciuonzo, D., De Maio, A., Foglia, G., *et al.*: 'Intrapulse radar-embedded communications via multiobjective optimization', *IEEE Trans. Aerosp. Electron. Syst.*, 2015, **51**, (4), pp. 2960–2974

[11] Wang, W.-Q.: 'MIMO SAR OFDM chirp waveform diversity design with random matrix modulation', *IEEE Trans. Geosci. Remote Sens.*, 2015, **53**, (3), pp. 1615–1625

[12] Babaei, A., Tranter, W.H., Bose, T.: 'A null space-based precoder with subspace expansion for radar/communications coexistence'. Proc. of Global Communications Conf., Atlanta, CA, December 2013, pp. 3487–3492

[13] Turlapaty, A., Jin, J.W.: 'A joint design of transmit waveforms for radar and communications systems in coexistence'. Proc. of IEEE Radar Conf., Cincinnati, OH, May 2014, pp. 315–319

[14] Ripplinger, D., Narula-Tam, A., Szeto, K.: 'Integrated radar and communications based on chirped spread-spectrum techniques'. Proc. of MTT-S Int. Microwave Symp., Phiadelphia, USA, June 2003, pp. 611–614

[15] Jamil, M., Zepernick, H.J., Pettersson, M.I.: 'On integrated radar and communication systems using Oppermann sequences'. Proc. of IEEE Int. Military Communications Conf., San Diego, November 2008, pp. 1–6

[16] Barrenechea, P., Elferink, F., Janssen, J.: 'FMCW radar with broadband communication capability'. Proc. of the 4th European Radar Conf., Munich, Germany, October 2007, pp. 130–133

[17] Settle, T.F., Picciolo, M.L., Goldstein, J.S.: 'Environmentally-shaped colored spreading sequences for robust wireless communications'. Proc. of Int. Waveform Diversity Design Conf., Niagara Falls, ON, August 2010, pp. 40–44

[18] Cheng, S.J., Wang, W.Q., Shao, H.Z.: 'Spread spectrum coded OFDM chirp waveform diversity design', *IEEE Sens. J.*, 2015, **15**, (10), pp. 5694–5700

[19] Wang, W.-Q.: 'MIMO SAR imaging: potential and challenges', *IEEE Aerosp. Electron. Syst. Mag.*, 2013, **27**, (8), pp. 18–23

[20] Donnet, B.J., Longstaff, I.D.: 'Combining MIMO radar with OFDM communications'. Proc. of 3rd European Radar Conf., Manchester, UK, September 2006, pp. 37–40

[21] Lellouch, G., Tran, P., Pribic, R., *et al.*: 'OFDM waveforms for frequency agility and opportunities for Doppler processing in radar'. Proc. of IEEE Radar Conf., Rome, May 2008, pp. 1–6

[22] Sturm, C., Zwick, T., Wiesbeck, W.: 'An OFDM system concept for joint radar and communications operation'. Proc. of IEEE 69th Vehicular Technology Conf., Barcelona, Spain, April 2009, pp. 1–5

[23] Thompson, S.C., Stralka, J.P.: 'Constant envelope OFDM for power-efficient radar and data communications'. Proc. of Int. Waveform Diversity and Design Conf., Kissimmee, FL, February 2009, pp. 291–295

[24] Garmatyuk, D., Kauffman, K., Schuerger, J., *et al.*: 'Wideband OFDM system for radar and communications'. Proc. of the IEEE Radar Conf., Pasadena, CA, May 2009, pp. 1–6

[25] Jung, B.W., Adve, R.S., Chun, J., *et al.*: 'Detection performance using frequency diversity with distributed sensors', *IEEE Trans. Aerosp. Electron. Syst.*, 2011, **47**, (3), pp. 1800–1812

[26] Wang, W.-Q.: 'Space-time coding MIMO-OFDM SAR for high-resolution remote sensing', *IEEE Trans. Remote Sens.*, 2011, **49**, (8), pp. 3094–3104

[27] Franken, G., Nikookar, H., Genderen, P.V.: 'Doppler tolerance of OFDM-coded radar signals'. Proc. of European Radar Conf., Manchester, UK, September 2006, pp. 108–111

[28] Sen, S.: 'PAPR-constrained pareto-optimal waveform design for OFDM-STAP radar', *IEEE Trans. Geosci. Remote Sens.*, 2014, **52**, (6), pp. 3658–3669

[29] Wang, W.-Q., Cai, J.Y.: 'MIMO SAR using chirp diverse waveform for wide-swath remote sensing', *IEEE Trans. Aerosp. Electron. Syst.*, 2012, **48**, (4), pp. 3171–3185

[30] Kim, J.H., Younis, M., Moreira, A., *et al.*: 'A novel OFDM chirp waveform scheme for use of multiple transmitters in SAR', *IEEE Geosci. Remote Sens. Lett.*, 2013, **10**, (3), pp. 568–572

[31] Wang, W.-Q.: 'MIMO SAR chirp modulation diversity waveform design', *IEEE Geosci. Remote Sens. Lett.*, 2014, **11**, (9), pp. 1644–1648
[32] Cheng, S.-J., Wang, W.-Q., Shao, H.Z.: 'OFDM radar waveform design with sparse modeling and correlation optimization'. Proc. of IEEE Geoscience and Remote Sensing Symp., Milan, Italy, July 2015, pp. 1–4
[33] Wang, W.-Q.: 'Mitigating range ambiguities in high PRF SAR with OFDM waveform diversity', *IEEE Geosci. Remote Sens. Lett.*, 2013, **10**, (1), pp. 101–105
[34] Cao, Y.-H., Xia, X.-G., Wang, S.-H.: 'IRCI-free colocated MIMO radar based on sufficient cyclic prefix OFDM waveforms', *IEEE Trans. Aerosp. Electron. Sys.*, 2015, **51**, (3), pp. 2107–2119
[35] Zhang, T.X., Xia, X.-G.: 'OFDM synthetic aperture radar imaging with sufficient cyclic prefix', *IEEE Trans. Geosci. Remote Sens.*, 2015, **53**, (1), pp. 394–404
[36] Sahai, A., Patel, G., Sabharwal, A.: 'Pushing the limits of full-duplex: design and real-time implementation', arXiv preprint,1107.0607, 2011, pp. 1–12
[37] Middleton, R.J.C.: 'Dechirp-on-receive linearly frequency modulated radar as a matched-filter detector', *IEEE Trans. Aerosp. Electron. Syst.*, 2012, **48**, (3), pp. 2716–2718
[38] Stinco, P., Greco, M.S., Gini, F., *et al.*: 'Ambiguity function and Cramer-Rao bounds for universal mobile telecommunications system-based passive coherent location systems', *IET Radar Sonar Navig.*, 2012, **6**, (7), pp. 668–678
[39] Colone, F., Woodbridge, K., Guo, H., *et al.*: 'Ambiguity function analysis of wireless LAN transmissions for passive radar', *IEEE Trans Aerosp. Electron. Syst.*, 2011, **47**, (1), pp. 240–264
[40] He, Q., Blum, R.S., Haimovich, A.M.: 'Noncoherent MIMO radar for location and velocity estimation: more antennas means better performance', *IEEE Trans. Signal Process.*, 2010, **58**, (7), pp. 3661–3680
[41] Gogineni, S., Rangaswamy, M., Rigling, B.D., *et al.*: 'Ambiguity function analysis for UMTS-based passive multistatic radar', *IEEE Trans. Signal Process.*, 2014, **62**, (11), pp. 2945–2957
[42] Tigrek, R.F., De Heij, W.J.A., Genderen, P.V.: 'OFDM signals as the radar waveform to solve Doppler ambiguity', *IEEE Trans. Aerosp. Electron. Syst.*, 2012, **48**, (1), pp. 130–143
[43] Sharif, M., Gharavi-Alkhansari, M., Khalaj, B.H.: 'On the peak-to-average power of OFDM signals based on oversampling', *IEEE Trans. Commun.*, 2003, **51**, (1), pp. 72–78

8 Appendix

According to (12), $E\{|\chi(\tau, f_d)|^2\}$ can be expressed as (21). Under the assumption of statistically independent symbols, similarly we have (see (21))

$$E\{a_{m,n}a^*_{m',n'}a^*_{m'',n''}a_{m''',''',n}\} = \begin{cases} \xi^2, & m=m', n=n', m''=m''', n''=n''' \\ \xi^2, & m=m'', n=n'', m'=m''', n'=n''', m\neq m', n\neq n \\ 0, & \text{else} \end{cases} \tag{22}$$

In this case, (21) can be further simplified into (23). According to (16), the terms in the first $\{\cdot\}$ can be rewritten in a closed-form expression (see (23))

$$\left|\frac{\sin(\pi(f_d-k_r\tau)(T_w-|\tau|))}{\pi(f_d-k_r\tau)}\right|^2\left|\frac{\sin(\pi(f_d-k_r\tau)N_sT_w)}{\sin(f_d-k_r\tau)T_w}\right|^2 \times\left|\frac{\sin(\pi N_c\Delta f\tau)}{\sin(\pi\Delta f\tau)}\right|^2. \tag{24}$$

and, the terms in the second $\{\cdot\}$ can be reformulated as (see (25)) Let $\tau'=\tau-(m-m')T_w$ and $f'_d=f_d-(n-n')\Delta f-k_r\tau$, (25) can be further simplified into

$$\begin{aligned} A(\tau,f_d) &= \sum_m\sum_n\sum_{m'\neq m}\sum_{n'\neq n}\int_{-\infty}^{\infty}\text{rect}\left(\frac{t}{T_w}\right)\text{rect}\left(\frac{t-\tau'}{T_w}\right)e^{-j2\pi f'_d t}dt \\ &\quad\times\int_{-\infty}^{\infty}\text{rect}\left(\frac{t'}{T_w}\right)\text{rect}\left(\frac{t'-\tau'}{T_w}\right)e^{j2\pi f'_d t'}dt' \\ &= |\chi_w(\tau-(m-m')T_w, f_d-(n-n')\Delta f+k_r\tau)|^2 \\ &= \sum_{m=-(N_s-1)}^{N_s-1}(N_s-m)\sum_{n=-(N_c-1)}^{N_c-1}(N_c-n) \\ &\quad\times|\chi_w(\tau-mT_w, f_d-n\Delta f+k_r\tau)|^2. \end{aligned} \tag{26}$$

Finally, (19) can be obtained by substituting (24) and (26) into (23).

$$\begin{aligned} E\{|\chi(\tau,f_d)|^2\} &= E\Bigg\{\sum_m\sum_n\sum_{m'}\sum_{n'}a_{m,n}a^*_{m',n'}\int_{-\infty}^{\infty}e^{j2\pi n\Delta f t+j\pi k_r t^2}\text{rect}\left(\frac{t-mT_w}{T_w}\right) \\ &\quad\times e^{-j2\pi n'\Delta f(t-\tau)-j\pi k_r(t-\tau)^2}\text{rect}\left(\frac{t-\tau-m'T_w}{T_w}\right)e^{-j2\pi f_d t}dt\sum_{m''}\sum_{n''}\sum_{m'''}\sum_{n'''}a^*_{m'',n''}a_{m''',n'''} \\ &\quad\times\int_{-\infty}^{\infty}e^{-j2\pi n''\Delta f t'-j\pi k_r t'^2}\text{rect}\left(\frac{t-m''T_w}{T_w}\right)e^{j2\pi n'''\Delta f(t'-\tau)+j\pi k_r(t'-\tau)^2}\text{rect}\left(\frac{t'-\tau-m'''T_w}{T_w}\right)e^{j2\pi f_d t'}dt'\Bigg\}. \end{aligned} \tag{21}$$

$$\begin{aligned} E\{|\chi(\tau,f_d)|^2\} &= \xi^2\Bigg\{\sum_m\sum_n\sum_{m''}\sum_{n''}\int_{-\infty}^{\infty}\text{rect}\left(\frac{t-mT_w}{T_w}\right)\text{rect}\left(\frac{t-\tau-mT_w}{T_w}\right)e^{j2\pi n\Delta f\tau}e^{-j2\pi(f_d-k_r\tau)t}dt \\ &\quad\times\int_{-\infty}^{\infty}\text{rect}\left(\frac{t'-m''T_w}{T_w}\right)\text{rect}\left(\frac{t'-\tau-m''T_w}{T_w}\right)e^{-j2\pi n''\Delta f\tau}e^{j2\pi(f_d-k_r\tau)t'}dt'\Bigg\} \\ &\quad+\xi^2\Bigg\{\sum_m\sum_n\sum_{m'}\sum_{n'}\int_{-\infty}^{\infty}\text{rect}\left(\frac{t-mT_w}{T_w}\right)e^{j2\pi n\Delta f t+j\pi k_r t^2}\text{rect}\left(\frac{t-\tau-m'T_w}{T_w}\right)e^{-j2\pi n'\Delta f(t-\tau)-j\pi k_r(t-\tau)^2}e^{-j2\pi f_d t}dt \\ &\quad\times\int_{-\infty}^{\infty}\text{rect}\left(\frac{t'-mT_w}{T_w}\right)e^{-j2\pi n\Delta f t'-j\pi k_r t'^2}\text{rect}\left(\frac{t'-\tau-m'T_w}{T_w}\right)e^{j2\pi n'\Delta f(t'-\tau)+j\pi k_r(t'-\tau)^2}e^{j2\pi f_d t'}dt'\Bigg\}. \end{aligned} \tag{23}$$

$$\begin{aligned} A(\tau,f_d) &= \sum_m\sum_n\sum_{m'\neq m}\sum_{n'\neq n}\int_{-\infty}^{\infty}\text{rect}\left(\frac{t}{T_w}\right)\text{rect}\left(\frac{t-\tau+(m-m')T_w}{T_w}\right)e^{j2\pi((n-n')\Delta f+k_r\tau)t}e^{-j2\pi f_d t}dt \\ &\quad\times\int_{-\infty}^{\infty}\text{rect}\left(\frac{t'}{T_w}\right)\text{rect}\left(\frac{t'-\tau+(m-m')T_w}{T_w}\right)e^{-j2\pi((n-n')\Delta f+k_r\tau)t'}e^{j2\pi f_d t'}dt' \end{aligned} \tag{25}$$